IEEE Sensors Letters Volume 2(3) (2017)

Heart Rate Monitoring during Physical Exercise from Photoplethysmography using Neural Network

Lianning Zhu[1], Chen Kan[2], Yuncheng Du[3], and Dongping Du[1]

[1] Department of Industrial, Manufacturing and Systems Engineering, Texas Tech University, Lubbock, TX 79409, USA
[2] Department of Industrial, Manufacturing and Systems Engineering, The University of Texas at Arlington, TX 76019, USA
[3] Department of Chemical and Biomolecular Engineering, Clarkson University, Potsdam, NY 13699, USA

Abstract— Photoplethysmography (PPG) signals have been widely used for heart rate (HR) monitoring. Compared to the electrocardiogram (ECG), PPG signals can be easily collected with wearable devices such as smart watches at a lower cost. However, PPG signals are often contaminated by the motion artifact (MA) and noises, which greatly deteriorate the signal quality and pose significant challenges on HR monitoring. In this paper, a new algorithm, using the spectral subtraction and the Neural Network (NN), is developed for accurate HR tracking in the presence of MA and noises. Specifically, the spectral component of MA is estimated from the acceleration (ACC) signals and then removed from the spectra of PPG. In addition, a NN model is developed based on new features extracted from ACC signals to identify the relationship between the ACC and HR variations in consecutive time windows. Such information is further used as a reference to select the spectral peak corresponding to the actual HR. A post-processing algorithm is used to correct mis-identified HR and to improve the accuracy. The NN-based algorithm is validated using the 2015 IEEE Signal Processing Cup Dataset. Our algorithm achieves an average absolute error of 1.03 beats per minutes (BPM) (standard deviation: 1.82 BPM), which outperforms previously reported works in the literature.

Index Terms— Photoplethysmography; Acceleration; Heart Rate Monitoring; Neural Network

I. INTRODUCTION

Heart rate (HR) is one of the most readily accessible and informative vital signs to evaluate cardiovascular conditions. For example, the elevated HR is an important risk factor associated with mortality and morbidity of patients with cardiovascular diseases [1]. Accurate HR monitoring is important in pre-diagnostics, rehabilitation, and disease prevention. HR is often measured using electrocardiogram (ECG) with multiple electrodes attached to the body surface. However, such an approach is not comfortable and often requires trained professionals to set up. For daily and continuous cardiac monitoring, photoplethysmography (PPG) has become a popular alternative to measure HR at a lower cost. PPG is typically measured by pulse oximeter imbedded in wearable devices, which captures the change in blood volume during cardiac cycles and the light intensity in tissues and other non-pulsatile blood [2]. Each cardiac cycle appears as a peak in the signal which reflects heart activities. However, PPG signals are oftentimes contaminated by the motion artifact (MA) resulting from the movements of subjects [3]. This, in turn, poses great challenges on accurate HR estimation.

Extensive studies have been conducted to eliminate MA from PPG signals to realize reliable HR monitoring. Popular methods include adaptive filter [4], Kalman filter [5], wavelet transform (WT) [6], singular spectrum analysis (SSA) [7], principal component analysis (PCA) [8], and independent component analysis (ICA) [3], empirical mode decomposition (EMD) [9], and spectrum subtraction (SS) [10]. Some of the studies use the motion data from the accelerometer, i.e., acceleration (ACC), as a reference to remove the MA. For example, Kalman filter can establish the relationships between PPG samples and ACC signals, and the model residuals are considered as clean PPG signals. Decomposition techniques such as WT and EMD can be used to separate the PPG signal into different components including clean PPG signals, noise, and MA, from which HR can be estimated. However, the performance of such methods can be affected by the decomposition and the component selection. For example, the choice of wavelets in WT, the size of trajectory matrix in SSA, and the stopping criterion of EMD can all affect the performance significantly.

Note that MA removal algorithm alone may not ensure a reliable HR tracking, since there are residual MA and noises in PPG signals. This may mislead the tracking algorithm and result in inaccurate estimation of HR. Techniques have been developed to accurately extract HR from PPG signals, which can be classified into three categories, i.e., spectral peak selection [11], dominant frequency calculation [12], and instantaneously frequency calculation [13]. For the spectral peak selection, Bayesian decision theory [10], support vector machine [14], and particle filter [15] were used to identify the peak corresponding to the actual HR. In addition, the dominant frequency of clean PPG signals was taken as the HR frequency [12]. For the instantaneously frequency method, Hilbert transform [16], phase vocoder technique [13], and short-time Fourier transform [17] were applied to estimate the HR. It is worth mentioning that previous studies focus on the identification of the spectral peaks corresponding to the actual HR, but only a few of them considers the impact of HR variation on the HR estimation. HR changes are correlated with the intensity of physical activities. For example, HR increases as the exercise intensity increases. However, limited work has been done to consider the correlation between the HR variation and subjects'

Corresponding author: D. Du (Dongping.du@ttu.edu)
Digital Object Identifier: 10.1109/LSEN.XXXX.XXXXXXX (inserted by IEEE).

motion in the tracking algorithm. The present study extracts the information pertinent to HR and HR variabilities from PPG and ACC signals, and further integrate them to improve the HR monitoring.

The proposed algorithm includes three consecutive steps: spectrum subtraction to remove MA, modeling of HR variations, spectral peak selection and HR estimation. First, PPGs and ACCs are transformed into the frequency domain and the maximum spectral peaks of ACCs are subtracted from the spectral of PPGs to remove MA. Note that the effect of MA on PPGs cannot be eliminated by the spectrum subtraction alone. To achieve a robust estimation of HR, a NN model is developed to predict the HR variation using new features extracted from the ACCs. The predicted variations are further used in the spectral peak selection to identify the actual HR. Finally, a post-processing algorithm is developed to correct the misidentified HR. Contributions of the present study include (*i*) the extraction of new features from the acceleration data, and (*ii*) the integration of predicted HR variations from the NN model into the HR tracking algorithm to facilitate an accurate HR estimation.

The paper is organized as follows. The method is present in Section II. Section III shows the efficiency of the proposed algorithm with a published dataset, followed by the conclusions in Section IV.

II. Methods

A. Preprocessing

The algorithm is validated using the 2015 IEEE Signal Processing Cup dataset of 12 subjects [8]. Recording for each subject includes one-channel ECG signals, two-channel PPG signals, and three-axis ACC signals. All signals are sampled at 125 Hz. Note that the goal in this current work is to develop an efficient PPG-based HR estimation algorithm, so ECG signals are used only for algorithm validation and the training of the neural network.

Before MA removal and HR estimation, the PPG and ACC signals are first filtered with a band-pass filter at 0.5 and 3 Hz to eliminate noises, and down-sampled to 25 Hz to reduce the computational cost. Then, a sliding time window is used to truncate the signal into small segments. The length of the time window is 8 s and the moving step is 2 s. In addition, PPG and ACC signals were normalized to ensure the variance is identical for all channels of ACC and PPG signals.

B. Motion Artifact Removal

Using ACCs, the spectral subtraction is performed to remove MA from PPG signals. To eliminate the impact of noises on the MA removal, we first examine the randomness of ACC signals, i.e., ACC signals that only contain random noises are excluded from the MA removal step. Then, PPG and the non-random ACC signals are transformed into the frequency domain, and the maximum spectrum of the ACC signals is removed from the spectra of the PPG signal. This is due to the fact that the spectra of the recorded PPG signals are proportional to the spectra of clean PPG and ACC signals [19].

Let define the spectra of PPG signals in a time window as: $\boldsymbol{x} = (x_1, x_2, \cdots, x_N)^T$, the spectra of transformed ACC signals as: $\boldsymbol{z} = (z_1, z_2, \cdots, z_N)^T$, and the spectra difference as: $\boldsymbol{y} = (y_1, y_2, \cdots, y_N)^T$, where $\boldsymbol{N}$ is the spectra length, the spectrum subtraction is defined as:

$$\boldsymbol{y} = \boldsymbol{x} - \boldsymbol{z} \tag{1}$$

Then, the spectra of the cleansed PPG signals can be obtained by setting the negative spectra difference to zero.

Using spectral subtraction, artifacts correlated to ACC signals can be removed. However, there are remaining noises and artifacts, which can still affect the HR tracking. As shown in Fig. 1, multiple peaks are observed in the frequency domain of PPG signals, which are attributed to ACC signals (blue triangle), HR (red circle), and noise (green square). MA removal technique may be able to eliminate the peak that corresponds to ACC, but the remaining noise (green square) can still mislead the HR estimation. It is important to distinguish the true peak from those of the noises and residual artifacts. To achieve this, we propose to infer HR variations from ACC signals and use the information to identify the actual HR.

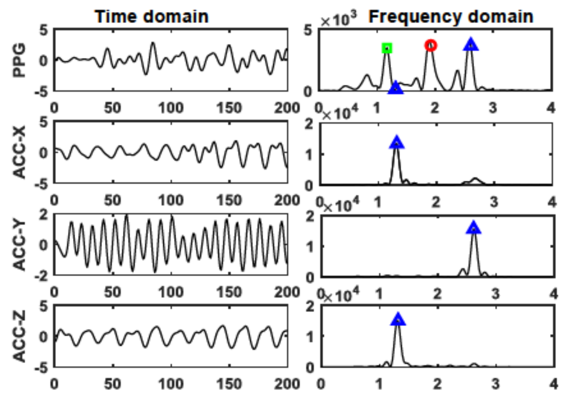

Figure 1. Time and frequency domain representation of PPG and ACC signals.

C. Modeling of HR Variations

HR variations are estimated by a NN model based on the features extracted from the ACC signals, which are further used to identify the spectral peaks corresponding to HR.

The NN model is developed using two types of features extracted from the ACC signals, i.e., the summation of the sum of the squared ACC signals in each time window (denoted as $S_{acc,i}$ in the ith time window), i.e., $S_{acc,i}=\sum_{j=1}^{n}(X_{acc,j}^2 + Y_{acc,j}^2 + Z_{acc,j}^2)$, and the rate of S_{acc} changes (denoted as $\boldsymbol{\beta_i}$) between neighbor time windows. Here, rate of S_{acc} changes in five consecutive windows preceding the current window (i.e., the $(i-5)^{th}$ to the i^{th}time windows) are considered. Therefore, $\boldsymbol{\beta_i}$ is 1×6 vector for the i^{th} time window. The rationale of choosing these features is as follows. First, a positive correlation is observed between the variations in S_{acc} and the HR. As shown in Fig.2 (a), the trajectory of the HR is consistent to the S_{acc} despite slightly differences in amplitudes. In addition, the scatter plot of β and HR variations shows a positive correlation in Fig. 2 (b). Both figures indicate that it is feasible to identify changes in HR using S_{acc} and $\boldsymbol{\beta}$. Such information is useful for developing efficient HR estimation algorithm to find the actual HR in the presence of noises and MA.

For the NN model, the features extracted from the ACC are used as inputs, $\boldsymbol{x}$, while HR variations among windows are the output, i.e., $\hat{\boldsymbol{r}}$. Notably, the input-output relationship is defined as $\hat{\boldsymbol{r}} = f(\boldsymbol{w}, \boldsymbol{x}, \boldsymbol{b})$, where $\boldsymbol{w}$ is an $n \times 7$ weight matrix, n is the number of windows for each subject, and $\boldsymbol{b}$ is the bias. Linear activation function is chosen and Levenberg–Marquardt algorithm is used in backpropagation to find the optimal solution. In this way, the HR variation in the i^{th} time window can be predicted using features ($S_{acc,i}$, and β_i) extracted from ACCs in the current and previous windows, i.e., $(i\text{-}5)^{th}$ to i^{th} windows, which can be used in the next step to identify the actual HR.

This article has been accepted for publication in a future issue of this journal, but has not been fully edited. Content may change prior to final publication. Citation information: DOI 10.1109/LSENS.2018.2878207, IEEE Sensors Letters

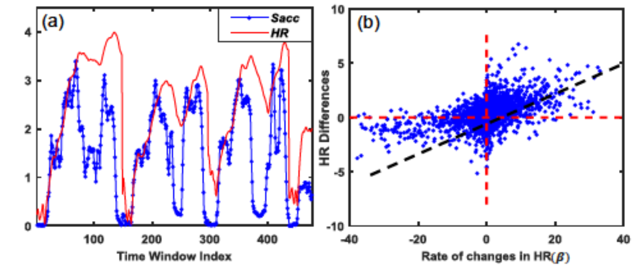

Figure 2. The correlation between S_{acc} and HR (a), and the correlation between β and HR variations (b).

D. HR Estimation

The HR in a time window can be decided by locating the maximum spectral peak. However, multiple peaks can be found in the PPG signals in the presence of MA and noises, which poses a great challenge on HR estimation. Identification of the correct spectral peak that corresponds to the actual HR is of great interest for robust HR tracking. To find the actual HR, the spectral peak is selected based on the predicted HR variations and selection criteria described as follows.

As seen in Fig. 3, we integrate the HR variations obtained from previous time windows (i.e., r_1, …, r_{i-1}) and the HR variations predicted with the NN model (i.e., $\hat{r}_1, \ldots, \hat{r}_{i-1}$) into a linear regression model to approximate the actual HR changes in the current time window. The algorithm proceeds as follows. (*i*) the HR changes ($\hat{r}_1, \ldots, \hat{r}_{i-1}$) in the previous windows are predicted using features extracted from ACC signals and the NN network model. (*ii*) The HR variations from previous windows (i.e., r_1, …, r_{i-1}) are calculated using the HR difference between two consecutive windows. (*iii*) Further, a linear regression model is developed to predict the actual HR change, r_i, in the i^{th} time window, from which the actual HR is predicted as $\widehat{hr_i} = hr_{i-1} + r_i$. The spectral peak that provides the closest estimation to $\widehat{hr_i}$ will be selected. Such a design balances the information between acceleration data and the previously estimated HRs, which in turn provides more reliable estimation.

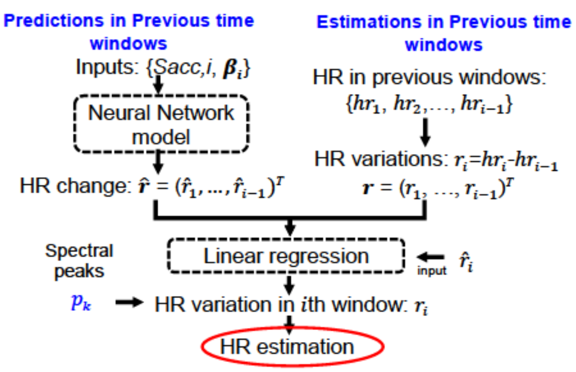

Figure 3. HR change prediction and HR estimation

Additional criteria are used to avoid incorrect estimation of HR. Specifically, spectral peaks whose amplitudes are less than 0.8 times of the maximum spectral amplitude will be discarded. A HR is treated as an incorrect estimation when it is 20 BPM higher than the HR estimations in two consecutive windows prior to the current window.

E. Post Processing

A moving average filter is used to post-process the HR estimations. Given the estimated HR hr_i, a window containing nearest 10 HRs is generated, and their mean and standard deviation are defined as m_r and σ_i, respectively. When the estimation (hr_i) is found to be inside the range of $[m_i - \sigma_i, m_i + \sigma_i]$, it is treated as the actual HR. Otherwise, it is considered inaccurate. Further, a smooth algorithm [18] is used to find the false estimation in all time windows. For the selected HR, $\boldsymbol{hr}$, the corrected HRs, $\boldsymbol{hr'}$, are given in a cost function:

$$S = |\boldsymbol{hr} - \boldsymbol{hr'}|^2 + \lambda|\boldsymbol{D}\boldsymbol{hr'}|^2 \tag{2}$$

where λ is a constant and $\boldsymbol{D}$ is a differential matrix. To minimize this cost function, partial derivatives of S with respect to $\boldsymbol{hr'}$ are used as:

$$\frac{\partial S}{\partial \boldsymbol{hr'}} = -2(\boldsymbol{hr} - \boldsymbol{hr'}) + 2\lambda \boldsymbol{D}^{\boldsymbol{T}}\boldsymbol{D}\boldsymbol{hr} \tag{3}$$

By setting (3) to 0, the corrected HRs, $\boldsymbol{hr'}$, can be calculated as:

$$\boldsymbol{hr'} = (\boldsymbol{I} + \lambda \boldsymbol{D}^{\boldsymbol{T}}\boldsymbol{D})^{-1}\boldsymbol{hr} \tag{4}$$

where $\boldsymbol{I}$ is an identity matrix and λ is set to 30. When the relative error between $\boldsymbol{hr}$ and corrected $\boldsymbol{hr'}$ is larger than 20%, the estimated HR was discarded and replaced by corresponding corrected HR.

Notably, it is expected that the detected HRs change smoothly and there is no large variation in a short period of time. Thus, piecewise polynomial is used to smooth the HR curve. This step is driven by the assumption that the HR varies continuously during physical exercise, and sharp changes are not likely to occur. Given the interval $[x_1, x_2]$, the false estimation is approximated by the polynomial function as:

$$f(x) = a(x - x_1)^3 + b(x - x_1)^2 + c(x - x_1)^1 + d \tag{5}$$

where a, b, c, and d are parameters obtained by fitting the estimated HR to the polynomial function.

III Results

To evaluate the proposed algorithm, two metrics are used, i.e., the average absolute error (Error1) and the average absolute error percentage (Error2). The former is defined as $e_1 = \left(\frac{1}{n}\right)\sum_{i=1}^{n}|r_{est,i} - r_{true,i}|$, while the latter is defined as $e_2 = \left(\frac{1}{n}\right)\sum_{i=1}^{n}\frac{|r_{est,i} - r_{true,i}|}{r_{true,i}}$. As seen in Table I, the proposed model achieves 1.03BPM and 0.79% for Error1 and Error2, respectively. Our error rates are lower than the error rates previously reported in [10] and [19], where Error1 and Error2 are 1.50BPM and 1.12BPM, 1.28% and 1.01%, respectively. In addition, the proposed algorithm in this current work can provide a lower standard deviation as compared to [10], i.e., 1.82 and 1.5 in our work *vs* 2.61 and 2.29 in [10].

It is worth mentioning that our method shows better performance on subject 10 and subject 12 as compared to other studies (see Table I). Fig. 4 shows the spectra of PPG signals of the subject 10 and 12 after MA removal, the actual HR (red solid line), and our estimations (red dotted line). Notably, the proposed algorithm can accurately estimate the HR when the spectral peak is dominated by noises (see the area circled by yellow).

Further, the efficiency of the proposed algorithm is graphically demonstrated using the Bland-Altman plot and the scatter plot between r_{true} and r_{est} with a fitted line, which indicates the errors between the estimated HR and the actual HR. The Bland-Altman plot shows the relationship between $(r_{true} + r_{true})/2$, and $(r_{true} - r_{true})$. As seen in Fig. 5 (a), the *x-axis* and *y-axis* of the Bland-Altman plot are the average of the difference between the actual HRs and the estimations. The 95% limit of agreement is [-2.55, 4.59] BPM. Scatter plot between BPM_{true} and BPM_{est} is given in Fig. 5 (b) with a fitted line $Y = 0.9947X + 0.7895$, where X is BPM_{true} and Y is BPM_{est}.

This article has been accepted for publication in a future issue of this journal, but has not been fully edited. Content may change prior to final publication. Citation information: DOI 10.1109/LSENS.2018.2878207, IEEE Sensors Letters

The correlation coefficient is 0.9969 and R^2 is 0.9950, indicating that the proposed algorithm can provide an accurate estimation of HR.

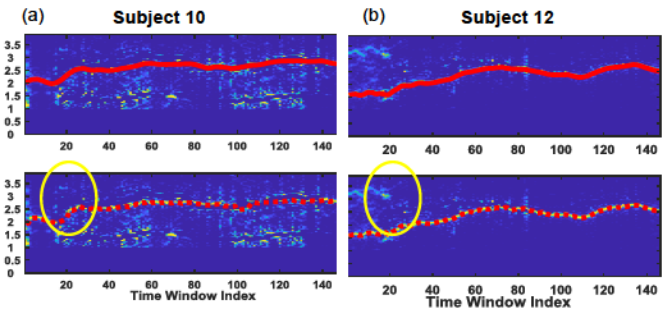

Figure 4. Spectra of PPG signals for subject 10 (left) and 12 (right). (Actual HR: red solid line, estimated HR: red dotted line)

Table I Errors of HR Estimation

No.	e_1 (BPM)			e_2 (%)		
	ALS [10]	*JOSS [19]*	*NN*	*ALS [10]*	*JOSS [19]*	*NN*
1	1.18	1.33	1.47	1.04	1.19	1.27
2	2.42	1.75	1.35	2.33	1.66	1.23
3	0.86	1.47	0.82	0.66	1.27	0.65
4	1.38	1.48	0.78	1.31	1.41	0.72
5	0.92	0.69	0.67	0.74	0.51	0.49
6	1.37	1.32	1.23	1.14	1.09	0.93
7	1.53	0.71	1.23	1.36	0.54	0.87
8	0.64	0.56	0.52	0.55	0.47	0.44
9	0.60	0.49	0.53	0.52	0.41	0.42
10	3.65	3.81	2.15	2.27	2.43	1.36
11	0.92	0.78	0.73	0.65	0.51	0.47
12	1.25	1.04	0.84	1.02	0.81	0.6
Avg.	1.50	1.28	1.03	1.12	1.01	0.79
s.d.	1.95	2.61	1.82	1.47	2.29	1.5

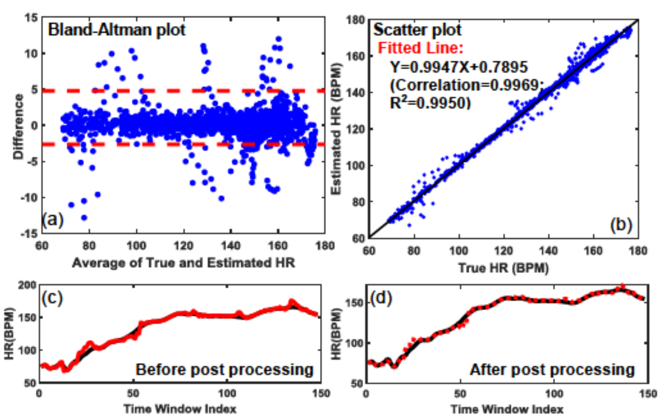

Figure 5. Performance of the proposed algorithm (a & b), and comparison of estimated HRs before (c) and after post processing (d).

To show the advantages of the linear regression for accurate HR estimation, experiment was conducted without the regression model. Error1 and Error2 are 1.13±2.13 and 0.86±1.67%, respectively, which shows the efficiency of the regression to improve HR estimation.

To explore the effect of post-processing on the HR estimation, a comparison between the actual HR with the estimated HR *before* and *after* the post-processing for subject 1 is shown in Fig. 5 (c) and (d). As seen, the post-processing can smooth the trajectory of HR and improve the accuracy of HR estimation. The efficiency of the algorithm is also evaluated in terms of computation time. Notably, an average of 1.185 s was required to process a subject (performed using Intel Core i5 CPU 650 @3.20 GHz and 8GB RAM).

IV CONCLUSION

PPG signals are oftentimes contaminated by MAs, which poses challenges on accurate HR estimation. This paper develops a new algorithm to efficiently identify the HR during physical exercise using PPG signals. Specifically, spectrum subtraction is firstly implemented to remove major components of MA from the PPG signals. Then, the neural network and a linear regression model are combined to identify the most possible spectral peaks from the spectra of cleansed PPG signals. Further, post-processing techniques are used to enhance the result of HR tracking. The efficiency of the proposed algorithm is evaluated on a benchmark dataset. Experimental results show that the proposed algorithm outperforms other methods previously reported.

ACKNOWLEDGMENT

The authors would like to thank the National Science Foundation (CMMI-1646664, CMMI-1728338, CMMI-1727487) for the financial supports on this study.

REFERENCES

[1] Palatini, P. and S. Julius, Elevated heart rate: a major risk factor for cardiovascular disease. Clin Exp Hypertens, 2004. 26(7-8): p. 637-44.
[2] Lee, H., et al., Wearable Multichannel Photoplethysmography Framework for Heart Rate Monitoring During Intensive Exercise. IEEE Sensors Journal, 2018. 18(7): p. 2983-2993.
[3] Kim, B.S. and S.K. Yoo, Motion artifact reduction in photoplethysmography using independent component analysis. IEEE transactions on biomedical engineering, 2006. 53(3): p. 566-568.
[4] Ye, Y., et al., Combining nonlinear adaptive filtering and signal decomposition for motion artifact removal in wearable photoplethysmography. IEEE Sensors Journal, 2016. 16(19): p. 7133-7141.
[5] Li, Q., R.G. Mark, and G.D. Clifford, Robust heart rate estimation from multiple asynchronous noisy sources using signal quality indices and a Kalman filter. Physiological measurement, 2007. 29(1): p. 15.
[6] Raghuram, M., et al. Evaluation of wavelets for reduction of motion artifacts in photoplethysmographic signals. 10th International Conference on Information Science, Signal Processing and their Applications (ISSPA 2010), Kuala Lumpur, 2010, pp. 460-463.
[7] Ye, Y., et al., A robust random forest-based approach for heart rate monitoring using photoplethysmography signal contaminated by intense motion artifacts. Sensors, 2017. 17(2): p. 385.
[8] Madhav, K.V., et al., Robust extraction of respiratory activity from PPG signals using modified MSPCA. IEEE Transactions on Instrumentation and Measurement, 2013. 62(5): p. 1094-1106.
[9] Sun, X., et al. Robust heart beat detection from photoplethysmography interlaced with motion artifacts based on empirical mode decomposition. Proceedings of 2012 IEEE-EMBS International Conference on Biomedical and Health Informatics, Hong Kong, 2012, pp. 775-778..
[10] Sun, B. and Z. Zhang, Photoplethysmography-based heart rate monitoring using asymmetric least squares spectrum subtraction and bayesian decision theory. IEEE Sensors Journal, 2015. 15(12): p. 7161-7168.
[11] Zhang, Z., Z. Pi, and B. Liu, TROIKA: A general framework for heart rate monitoring using wrist-type photoplethysmographic signals during intensive physical exercise. IEEE Transactions on Biomedical Engineering, 2015. 62(2): p. 522-531.
[12] Motin, M.A., C.K. Karmakar, and M. Palaniswami, Ensemble empirical mode decomposition with principal component analysis: a novel approach for extracting respiratory rate and heart rate from photoplethysmographic signal. IEEE journal of biomedical and health informatics, 2018. 22(3): p. 766-774.
[13] Temko, A., Accurate heart rate monitoring during physical exercises using ppg. IEEE Transactions on Biomedical Engineering, 2017. 64(9): p. 2016-2024.
[14] Xiong, J., et al., SVM-based spectral analysis for heart rate from multi-channel WPPG sensor signals. Sensors, 2017. 17(3): p. 506.
[15] Fujita, Y., M. Hiromoto, and T. Sato, PARHELIA: Particle Filter-Based Heart Rate Estimation From Photoplethysmographic Signals During Physical Exercise. IEEE Transactions on Biomedical Engineering, 2018. 65(1): p. 189-198.
[16] Jarchi, D. and A.J. Casson, Towards photoplethysmography-based estimation of instantaneous heart rate during physical activity. IEEE Transactions on Biomedical Engineering, 2017. 64(9): p. 2042-2053.
[17] Zhao, D., et al., Sfst: A robust framework for heart rate monitoring from photoplethysmography signals during physical activities. Biomedical Signal Processing and Control, 2017. 33: p. 316-324.
[18] Eilers, P.H.C., A Perfect Smoother. Analytical chemistry, 2003. 75(14): p. 3631-3636.
[19] Zhang, Z., Photoplethysmography-based heart rate monitoring in physical activities via joint sparse spectrum reconstruction. IEEE transactions on biomedical engineering, 2015. 62(8): p. 1902-1910.